JOURNAL OF ENGINEERING SCIENCES

Volume 10, Issue 1 (2024)

Goroshko A. V., Zembytska M. V., Paiuk V. P. (2024). Induction motor vibrations caused by mechanical and magnetic rotor eccentricity. Journal of Engineering Sciences (Ukraine), Vol. 11(1), pp. D66–D77. https://doi.org/10.21272/jes.2024.11(1).d8

Induction Motor Vibrations Caused by Mechanical and Magnetic Rotor Eccentricity

Goroshko A. V.*[0000-0002-1386-2326], Zembytska M. V.[0000-0002-6671-9937], Paiuk V. P.[0000-0002-9969-8239]

Khmelnytskyi National University, 11, Instytutska St., 29016 Khmelnytskyi, Ukraine

Article info:

Submitted:	January 12, 2024
Received in revised form:	April 16, 2024
Accepted for publication:	April 30, 2024
Available online:	May 3, 2024

***Corresponding email:**
horoshkoan@khmnu.edu.ua

Abstract. Vibration reduction of induction motors is a significant problem that requires effective models for the effects of mechanical and electromagnetic unbalanced forces. This article presents a mathematical model of dynamics for induction motors with rotor mass eccentricity and static and dynamic magnetic eccentricity. The model allows for the influence of the gyroscopic torque of the rotor and considers the elastic-damping characteristics of each of the stator supports and their location. The model has eight degrees of freedom, which makes it possible to simulate transverse and axial vibrations of various designs' rotors and housings of induction motors. The results of modeling the dynamics for a three-phase squirrel cage induction motor with 11 kW capacity agreed with those obtained by other authors. Simultaneously, new results were also obtained within the research. The simulation results showed that the static magnetic eccentricity causes the appearance of additional critical speed of the motor, and its value decreases in proportion to the growth of the number of pole pairs. The change of the moment of inertia of the motor at a mismatch of the main axis of symmetry of the stator and the rotor axis of rotation allowed for obtaining an actual frequency spectrum of free oscillations, including the rotational motion of the stator. Since the actual static magnetic eccentricity can additionally increase at operating frequencies due to the increase of bearing clearance caused by dynamic unbalanced load, it should be considered in the analysis of unbalanced magnetic pull. The angle of static magnetic eccentricity significantly affects the magnitude of radial vibrations. This feature should also be considered when selecting the locations of balancing weights during the rotor balancing procedure.

Keywords: induction motor, eccentricity of rotor mass, magnetic eccentricity, unbalanced magnetic pull, axial vibration, process innovation.

1 Introduction

Due to their high operational efficiency, induction machines are among the most commonly used engines in various industrial fields [1]. For induction machines, bearings fixed in special risers are applied to support the rotor. The risers are bolted to the lower half of the end shield. Induction machine bearing failures account for about 40 % of the total number of failures [2, 3]. Bearing failures are mainly caused by their increased wear. The main wear factors are rotor mechanical unbalance due to rotor mass eccentricity and unbalanced magnetic pull (UMP) due to magnetic eccentricity. Since induction machines have a relatively small air gap, they are more susceptible to UMP. The dynamic forces and moments caused by rotor eccentricity are additional internal excitations for the motor subsystem, which include centrifugal force, friction-impact force, UMP, unbalanced force torque, and friction torque [4].

Mechanical unbalance occurs due to inevitable technological deviations during manufacturing, assembly inaccuracy, and rotor design features. Consequently, axial symmetry is broken, and the center of inertia in some cross-sections does not coincide with the geometric center of sections and the rotor rotation axis. Magnetic eccentricity and UMP cause additional radial force on the bearing, which reduces its service life. In addition, UMP reduces the overall stiffness of the system, which can increase vibrations within the system [5].

2 Literature Review

According to various sources, eccentricity accounts for 20–40 % of induction motor (IM) failures [6, 7]. Rotor eccentricity often occurs in IMs, leading to non-uniformity of the machine's air gap [8, 9]. Magnetic eccentricity occurrence is caused by errors in the production and assembly of the machine and unfavorable conditions of its

operation. A distinction is made between static and dynamic eccentricity. Static eccentricity is caused by the eccentric position of the rotor in the stator bore, so the uneven configuration of the air gap does not change in time as the rotor rotates. The static eccentricity of the air gap should not exceed 10 % [4].

At dynamic eccentricity, which occurs due to the eccentric position of the rotor relative to the shaft axis, the configuration of the air gap changes during rotor rotation, which is caused by the rotation of the rotor axis relative to the stator axis. Due to the small size of the air gap of the IM, even a small eccentricity of the rotor, breaking the symmetry of the machine design, significantly worsens its performance.

Therefore, timely detection of eccentricity in the early stages of its development is of great practical importance, and it is one of the essential tasks of monitoring the technical condition of the IM and diagnosing its defects.

The most effective method is electromagnetic vibration diagnostics – monitoring and analysis of changes in the IM vibrations of electromagnetic origin depending on the type and degree of eccentricity development [10].

Both analytical approaches to UMP analysis and methods based on the finite element method are known [11, 12]. In general, it is necessary to consider separately the influence of static rotor mass eccentricity and static rotor eccentricity, which is the cause of the non-uniformity of the air gap of the electric machine. In the worst case, the centrifugal force caused by rotor unbalance and radial vibration-inducing force of an electromagnetic nature can add up and cause increased IM vibrations.

Therefore, some authors [13–15] conducted research works to create mathematical models that would most effectively describe the rotor dynamics of an IM. Chuan and Shek propose monitoring systems for the online detection of faults due to eccentricity due to unbalanced magnetic tension in induction machines [10]. Werner analyzed the analytical model and steady motion sections of rotating machines whose "feet" are mounted on a pliable foundation [16]. Werner explained how to consider electromagnetic field damping and established an analytical model of vibration of the IM housing and shaft is considered, considering dynamic mass eccentricity, deflection of the deformed shaft, and magnetic eccentricity for an IM with sliding bearings mounted on a pliable foundation [17].

Other researchers investigated the effect of static, dynamic, and mixed eccentricity of an electric machine [18–20]. Du and Li studied an analytical method for calculating the UMP in a rotating coordinate system [21]. Lei et al. [22] conducted a study where the electromagnetic force waves and vibration response at air gap eccentricity were calculated using an analytical approach and the finite element method (FEM). They quantitatively analyzed the effect of eccentricity on the electromagnetic force wave and vibration response of a squirrel cage motor.

Essen [23] used fractional order in the finite element model to analyze the harmonic response. As a result, an optimal design for the rotor of a traction IM for transport was proposed.

The duration of its operation and the frequency of unplanned maintenance depend on how the IM is mounted on a special welding structure, a reinforced foundation with a mortgage frame, or concrete anchors. In order to correctly and reliably fix the electric motor, it is necessary to consider the location of the bearings and shaft ends relative to the fastening elements and the spatial position of the machine relative to the driven mechanism. The most common engines in the industry are the engines with feet on the body, the ones with feet and a flange on one or both bearing shields, and those without feet with a flange on a bearing shield or shields. Studies [16–18] show a yielding foundation's influence on the rotor dynamics.

In the models considered in the research mentioned earlier, it is assumed that inertia is concentrated in a plane, dividing the length of the rotor in half, and eccentricity causes a centrifugal force under which the rotor carries out only translational movements. In contrast to such works, this article set the task of developing a model with an arbitrary location of the center of mass and the magnetic center of the rotor. This will allow us to consider the static mass imbalance and the magnetic eccentricity of the rotor, taking into account the torques of the imbalance force and, accordingly, the rotational movements of the stator. In the proposed model, a rigid motor stator housing must have 6 degrees of freedom (DOF) and can perform translational motion in the directions of the *x*, *y*, and *z* axes, as well as rotations around these axes.

The purpose of this article is to create a mathematical model of oscillations of the IM housing, which would allow for the eccentricity of the rotor mass, the static magnetic eccentricity of the rotor, the influence of the gyroscopic moment of the rotor, and the rigidity of the stator supports to the foundation, allowing 6 DOF (three translational and three rotational); taking into account the unequal rigidity of the stator supports, their number and places of connection to the stator; general case of spatial mismatch of the centers of mass of the stator and rotor with the axis of rotation along all three axes *x*, *y*, *z*.

3 Research Methodology

3.1 Considering the eccentricity of the rotor

In the proposed model, the absolutely rigid motor stator housing has six degrees of freedom and can perform translational motion in the directions of the *x*, *y*, and *z* axes, as well as rotations around these axes. The rotor, rotating at a constant angular velocity ω, can make small translational movements in the direction of the *x* and *z* axes, having 2 DOF. Since the rotor movement is independent of the stator movement, the stator-rotor system has 8 DOF in total.

In the model shown in Fig. 1, the following assumptions are made:

– the elastic characteristics of all supports are linear;

– the rotor is considered rigid, and its deformations are neglected;

– the position of the rotor center of mass m_C is known.

To specify the stator position in this system's space, it is necessary to have 8 generalized coordinates. For such coordinates, we will take Cartesian coordinates of the stator center of inertia x, y, z, angles α, β, γ, which specify the rotations of these coordinate axes rigidly connected to the stator and two coordinates of the rotor center of inertia x_r and z_r. In these coordinates, stator oscillations can be represented as a superposition of six screw movements with fixed screw axes x, y, z. The stator generally performs six-circuit oscillations. The mass eccentricity is equal to $e_U = SD$, where point $D(x_D, y_D, z_D)$ is obtained due to the intersection of the rotor rotation axis with a plane drawn through the mass center S perpendicular to the rotation axis. Distance DO equals the distance from the rotation axis to the stator's center of mass. The distance from point D to the central axis of the stator's symmetry will be considered static magnetic eccentricity $e_{ms} = \sqrt{x_D^2 + z_D^2}$.

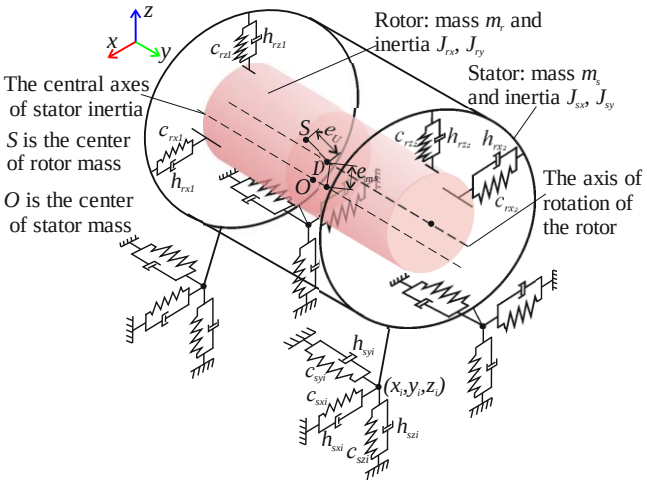

Figure 1 – Dynamic model of an IM with rotor mass eccentricity

The movement of the stator-rotor system can be considered as the movement of the moving coordinate system $a_1b_1c_1$ relative to the fixed xyz (Fig. 2).

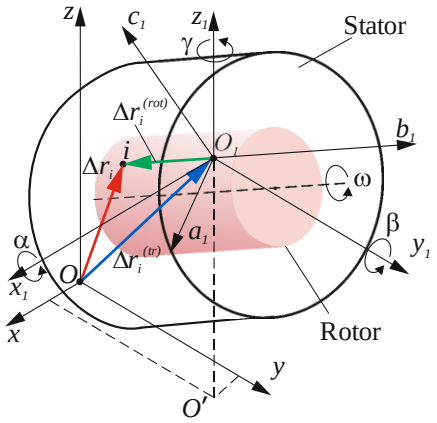

Figure 2 – Calculation diagram of the stator-rotor system

In the initial position at $\omega = 0$, both coordinate systems coincide. We assume that the center of mass of the stator O_1 does not lie on the rotation axis.

For a separate study of the translational and rotating motion of the stator, consider an additional coordinate system $x_1y_1z_1$ with a translationally moving center O_1, the axes of which, during movement, always remain parallel to the corresponding fixed axes of the xyz coordinate system.

The position of the moving system $a_1b_1c_1$ relative to the stationary system xyz will be determined by the coordinates of its pole $O_1(x, y, z)$ and the angles α, β, γ of rotations of the coordinate system $a_1b_1c_1$ around the translationally moving axes x_1, y_1, z_1. It also can be considered the coordinates x, y, z of point O_1, the rotation angles α, β, γ and coordinates a_1, c_1 of the system $a_1b_1c_1$ to be generalized coordinates.

3.2 Determination of stator movements

The displacement $\Delta\bar{r}_i$ of an arbitrary i-th point of the stator associated with the moving system of axes a_1, b_1, c_1 is the sum of displacement vectors during translational $\Delta\bar{r}^{(tr)}$ and rotational motion $\Delta\bar{r}_i^{(rot)}$. The translational vector looks like this:

$$\Delta\bar{r}^{(tr)} = x\bar{\imath} + y\bar{\jmath} + z\bar{k}, \qquad (1)$$

where x, y, z – displacement projections onto fixed coordinate axes; $\bar{\imath}, \bar{\jmath}, \bar{k}$ – unit vectors along these axes.

The displacement vector due to rotational motion $\Delta\bar{r}_i^{(rot)}$ of the i-th point of the stator is equal to

$$\Delta\bar{r}_i^{(rot)} = \bar{\psi} \times \bar{r}_i^{(rot)} = (\beta z_{1i} - \gamma y_{1i})\bar{\imath} + \\ +(\gamma x_{1i} - \alpha z_{1i})\bar{\jmath} + (\alpha y_{1i} - \beta x_{1i})\bar{k}, \qquad (2)$$

where $\bar{\psi}$ – the vector of the small angle of rotation of the system $a_1b_1c_1$ relative to x_1, y_1, z_1 axes; $\bar{r}_i^{(rot)}$ – the position vector of the i-th point relative to the origin O_1.

The projections of the total displacement Δr_i and velocity $\Delta\dot{r}_i$ of the i-th point, considering expressions (1) and (2), are as follows:

$$\begin{cases} \Delta r_{xi} = x + \beta z_{1i} - \gamma y_{1i}; \\ \Delta r_{yi} = y + \gamma x_{1i} - \alpha z_{1i}; \\ \Delta r_{zi} = z + \alpha y_{1i} - \beta x_{1i}; \end{cases} \Rightarrow \begin{cases} \Delta\dot{r}_{xi} = \dot{x} + \dot{\beta} z_{1i} - \dot{\gamma} y_{1i}; \\ \Delta\dot{r}_{yi} = \dot{y} + \dot{\gamma} x_{1i} - \dot{\alpha} z_{1i}; \\ \Delta\dot{r}_{zi} = \dot{z} + \dot{\alpha} y_{1i} - \dot{\beta} x_{1i}. \end{cases} \qquad (3)$$

3.3 Determination of the kinetic energy of the stator-rotor system

Let's m_s – the stator mass; $J_{a_1}^{(s)}$, $J_{b_1}^{(s)}$, and $J_{c_1}^{(s)}$ – the moments of inertia of the stator relative to the principal central axes a_1, b_1, c_1, respectively; m_r – the mass of the rotor; $J_{a_2}^{(r)}$, $J_{b_2}^{(r)}$, and $J_{c_2}^{(r)}$ – the moments of inertia of the rotor relative to the principal central axes a_2, b_2, c_2, respectively $\left(J_{a_2}^{(r)} = J_{c_2}^{(r)}\right)$. Therefore, the kinetic energy of the stator is defined using the König's theorem[23]:

$$T_s = \frac{1}{2}[m_s(\dot{x}^2 + \dot{y}^2 + \dot{z}^2) + \\ J_{a_1}^{(s)}\dot{\psi}_{a_1}^2 + J_{b_1}^{(s)}\dot{\psi}_{b_1}^2 + J_{c_1}^{(s)}\dot{\psi}_{c_1}^2], \qquad (4)$$

where $\dot{x}, \dot{y}, \dot{z}$ – the projections of the translational velocity on the x, y, z axes; $\dot{\psi}_{a_1}$, $\dot{\psi}_{b_1}$, and $\dot{\psi}_{c_1}$ – the

projections of the angular velocity vector $\overline{\psi} = \overline{\dot{\alpha}} + \overline{\dot{\beta}} + \overline{\dot{\gamma}}$ on the axes a_1, b_1, and c_1, respectively.

To formulate an expression for the rotor's kinetic energy, let us consider its motion in the general case (Fig. 3) when the center of the rotor mass *S* does not coincide with the stator center of mass *O*.

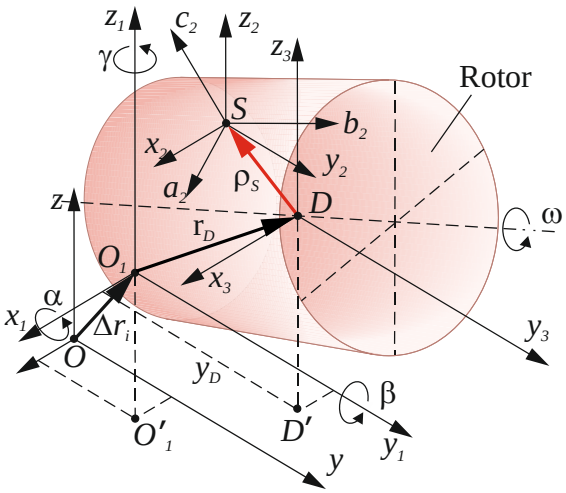

Figure 3 – Rotor displacement diagram

Let's consider additional coordinate systems: translationally moving $x_2y_2z_2$ with origin at *S* and coordinate system $x_3y_3z_3$ with origin at *D*, as well as rigidly connected with the rotor system $a_2b_2c_2$ with origin at *S* and system $a_3b_3c_3$ with origin at *D*. The axes of system $a_2b_2c_2$ will be considered as the main central axes of inertia of the rotor. At absence of eccentricity (e_U= 0) point *S* coincides with point *D*, axis a_2 coincides with axes x_2, a_3, x_3; axis b_2 coincides with axes y_2, b_3, y_3, axis c_2 coincides with axes z_2, c_3, z_3. It considered that in the initial state, the axes *y*, y_1, y_2, y_3 and b_1, b_2, b_3 are parallel to the rotor rotation axis.

A case of static mass unbalance occurs if $DO = 0$, but the center of mass of the rotor lies outside the rotational axis and $e_U = SD \neq 0$. The causes of such unbalance of the rotor are manufacturing errors or its deformation during operation, e.g., thermal deformation.

In the case of $e_U \neq 0$ and $y_D \neq 0$, there is a case of torque unbalance of the rotor. In practice, a solid rotor, such as the rotor of an IM, is characterized by dynamic unbalance. Due to the eccentric position of the rotor in the stator bore, the rotor rotation axis and the main central axis of inertia of the stator do not coincide: $x_D \neq 0$, $y_D \neq 0$, $z_D \neq 0$. The effect of unbalance is accounted for by considering the eccentricity e_U and the coordinates of the point *D* in the stationary coordinate system.

In the adopted coordinate system, the rotor motion, in general, can be represented as a complex one: translational motion with the center of mass *S* and rotation around this center of mass with the angular velocity of $\overline{\Omega} = \overline{\psi} + \overline{\omega}$.

The translational velocity of a point *S* is the sum of translational velocities of displacements:

$$\bar{V}_S = \bar{V}_{DO} + \bar{V}_{SD} = \left(\bar{V}_{O_1} + \bar{V}_{DO_1}\right) + \bar{V}_{SD}, \qquad (5)$$

where $\bar{V}_{DO}$ – absolute velocity of the pole *D* in system *xyz* relative to the pole *O*; $\bar{V}_{O_1}$ – the transfer velocity of the stator center of mass O_1 (stator velocity in the *xyz* system); $\bar{V}_{DO_1}$ – the relative velocity of the pole *D* (rotor velocity relative to the stator center of mass O_1); $\bar{V}_{SD}$ – the velocity of the center of mass *S* of the rotor in the coordinate system $x_3y_3z_3$ relative to the pole *D*.

Applying the König's theorem, the expression for the kinetic energy of the rotor has the form:

$$T_r = \frac{1}{2}\left[m_r(V_{Sx}^2 + V_{Sy}^2 + V_{Sz}^2) + J_{a_2}^{(2)}(\Omega_{a_2}^2 + \Omega_{c_2}^2) + J_{b_2}^{(2)}\Omega_{b_2}^2\right]. \qquad (6)$$

The kinetic energy *T* of the IM system is the sum of stator kinetic energy T_s and rotor kinetic energy T_r.

Denoting $\bar{V}_{O_1} = \dot{x}\bar{\imath} + \dot{y}\bar{k} + \dot{z}\bar{k}$, $\bar{V}_{DO_1} = \dot{x}_r\bar{\imath} + \dot{z}_r\bar{k}$, and using expressions (4) and (6), limiting the values of the second order of smallness, it can be obtained:

$$\begin{aligned} T_r = {} & \frac{m}{2}\left(\dot{x}^2 + \dot{y}^2 + \dot{z}^2\right) + \\ & + \frac{1}{2}\left(J_{a_1}\dot{\alpha}^2 + J_{b_1}\dot{\beta}^2 + J_{c_1}\dot{\gamma}^2\right) + \\ & + m_r\dot{x}\left(\dot{\beta}z_D - \dot{\gamma}y_D + \omega e_U \cos\omega t\right) - \\ & m_r\dot{\gamma}y_D\left(\dot{\beta}z_D + \omega e_U \cos\omega t\right) + \\ & + m_r\dot{\beta}\omega e_U(z_D \cos\omega t + x_D \sin\omega t) + \\ & m_r\omega^2 e_U^2 \cos^2\omega t + m_r\dot{y}(\dot{\gamma}x_D - \dot{\alpha}z_D) - \\ & - m_r\dot{\gamma}\dot{\alpha}x_D z_D + \frac{m_r}{2}(x_r^2 + z_r^2) + \\ & + m_r\dot{z}\left(\dot{\alpha}y_D - \dot{\beta}x_D - \omega e_U \sin\omega t\right) - \\ & - m_r\dot{\alpha}y_D\left(\dot{\beta}x_D + \omega e_U \sin\omega t\right) + \\ & \frac{1}{2}I_{b_2}^{(r)}\omega\left[\omega + 2\left(\dot{\beta} + \alpha\dot{\gamma} - \dot{\alpha}\gamma\right)\right] + \\ & + m_r\left[\dot{z}\dot{z}_r + \dot{x}_r\left(\dot{\beta}z_D - \dot{\gamma}y_D\right) + \right. \\ & + \dot{z}_r\left(\dot{\alpha}y_D - \dot{\beta}x_D\right) + \dot{x}\dot{x}_r + \\ & \left. + \omega e_U(\dot{x}_r \cos\omega t - \dot{z}_r \sin\omega t)\right], \end{aligned} \qquad (7)$$

where $m = m_s + m_r$ – the mass of the stator-rotor system; $J_{a_1} = J_{a_1}^{(s)} + J_{a_2}^{(r)} + m_r(y_D^2 + z_D^2)$ – the main moment of inertia of the system with respect to the axis a_1; $J_{b_1} = J_{b_1}^{(s)} + J_{b_2}^{(r)} + m_r(z_D^2 + x_D^2)$ – the main moment of inertia of the system with respect to the axis b_1; $J_{c_1} = J_{c_1}^{(s)} + J_{c_2}^{(r)} + m_r(x_D^2 + y_D^2)$ – the main moment of inertia of the system with respect to the axis c_1.

3.4 Determination of potential energy and dissipation energy of the system

Elastic deformations of the supports determine the system's potential energy during oscillations. Let the stator be connected to the foundation through *n* elastic elements and *m* dampers. To simplify the dependencies, let us assume that $n = m$ and the principal axes of stiffnesses and viscous friction constants of all elastic elements or dampers are parallel to the system's principal central axes of inertia.

The potential energy U of the stator-rotor system is the sum of the potential energy U_s stored in n stator supports and potential energy U_r stored in two rotor bearings:

$$U = U_S + U_r = \\ = \frac{1}{2}\sum_1^n\left(c_{sx_i}\Delta r_{x_i}^2 + c_{sy_i}\Delta r_{y_i}^2 + c_{sz_i}\Delta r_{z_i}^2\right) + \\ + \frac{1}{2}\sum_1^2\left(c_{rx_i}\Delta r_{x_i}^2 + c_{rz_i}\Delta r_{z_i}^2\right), \quad (8)$$

where Δr_{x_i}, Δr_{y_i}, and Δr_{z_i} – displacements along the x, y, and z axes of the points of connection of the stator support elastic elements to the moving system; c_{sx_i}, c_{sy_i}, and c_{sz_i} – projections of the stiffness vector of the i-th elastic element of the stator support; Δr_{rx_i} Δr_{rz_i} – relative displacements along the axes a_1, b_1, c_1 of the points of connection to the supports; c_{rx_i}, c_{rz_i} – projections of the stiffness vector of the i-th elastic element of the bearing support.

Considering (3), the dependence (8) takes the form:

$$U = \frac{1}{2}\sum_1^n\left[c_{sx_i}(x + \beta z_i - \gamma y_i)^2 + \right. \\ + c_{sy_i}(y + \gamma x_i - \alpha z_i)^2 + \\ \left. + c_{sz_i}(z + \alpha y_i - \beta x_i)^2\right] + \\ + \frac{1}{2}\sum_1^2\left(c_{rx_i}x_r^2 + c_{rz_i}z_r^2\right). \quad (9)$$

The dissipation of mechanical energy D in the system supports due to viscous friction can be represented as the sum of the damping energy D_s of the stator supports and the rotor bearing energy D_r:

$$D = D_S + D_r = \\ = \frac{1}{2}\sum_1^n\left(h_{sx_i}\Delta\dot{r}_{x_i}^2 + h_{sy_i}\Delta\dot{r}_{y_i}^2 + h_{sz_i}\Delta\dot{r}_{z_i}^2\right) + \\ + \frac{1}{2}\sum_1^2\left(h_{rx_i}\Delta\dot{r}_{rx_i}^2 + h_{rz_i}\Delta\dot{r}_{rz_i}^2\right), \quad (10)$$

where h_{sx_i}, h_{sy_i}, and h_{sz_i} – the projections of the vector of the viscous friction constant of the i-th stator support; $\Delta\dot{r}_{x_i}$, $\Delta\dot{r}_{y_i}$, and $\Delta\dot{r}_{z_i}$ – velocities along the x, y, and z axes of the points of connection of supports to the stator; h_{rx_i} and h_{rz_i} – the projections of the vector projections of the vector of the viscous friction constant of bearing arrangements; $\Delta\dot{r}_{rx_i}$ and $\Delta\dot{r}_{rz_i}$ – the relative velocities along the axes a_1, b_1, c_1 the points of support connection to the rotor.

After considering (3), dependence (10) takes the form:

$$D = \frac{1}{2}\sum_1^n\left[h_{sx_i}\left(\dot{x} + \dot{\beta}z_i - \dot{\gamma}y_i\right)^2 + \right. \\ + h_{sy_i}(\dot{y} + \dot{\gamma}x_i - \dot{\alpha}z_i)^2 + \\ \left. + h_{sz_i}\left(\dot{y} + \dot{\alpha}y_i - \dot{\beta}x_i\right)^2\right] + \\ + \frac{1}{2}\sum_1^2\left(h_{rx_i}\dot{x}_r^2 + h_{rz_i}\dot{z}_r^2\right).$$

3.5 Mathematical model of motor vibrations with rotor mass eccentricity

The differential equations of oscillations of the IM system are obtained from the Lagrange equation of the 2nd kind, considering energy dissipation at Rayleigh damping:

$$\frac{d}{dt}\left(\frac{\partial T}{\partial\dot{q}_j}\right) - \frac{\partial T}{\partial q_j} + \frac{\partial U}{\partial q_j} + \frac{\partial D}{\partial\dot{q}_j} = 0, \quad (11)$$

where $j = 1, 2, \ldots, 8$ – the number of generalized coordinates; T and U – the kinetic and potential energy of the system, respectively; D – a dissipative function describing energy dissipation in the system dampers due to viscous friction.

Performing mathematical operations provided by the Lagrange equation (11) on eight generalized coordinates x, y, z, α, β, γ, x_r, and z_r, putting ω = const, a system of 8 differential equations can be obtained, which in matrix form has the following form:

$$\boldsymbol{M}\ddot{\boldsymbol{q}} + (\boldsymbol{G} + \boldsymbol{D})\dot{\boldsymbol{q}} + \boldsymbol{A}\boldsymbol{q} = \mathbf{Q}, \quad (12)$$

where $\mathbf{q} = [x, y, z, \alpha, \beta, \gamma, x_r, z_r]^T$ – vector of generalized coordinates; $\mathbf{Q} = [F_x, 0, F_z, M_x, M_y, M_z, F_x, F_z]^T$ – vector of generalized force factors; $\boldsymbol{M} = \left[m_{ij}\right]_1^8$, $\boldsymbol{G} = \left[g_{ij}\right]_1^8$, $\boldsymbol{D} = \left[d_{ij}\right]_1^8$, and $\boldsymbol{A} = \left[\alpha_{ij}\right]_1^8$ – the inertia, gyroscopic, damping, and stiffness matrices, respectively.

3.6 Analysis of motor vibration model with rotor eccentricity

Analysis of equation (12) shows that for the lowest vibration activity of the IM in the presence of rotor mass eccentricity $e_U \neq 0$, it is necessary that matrices **M**, **D**, and **A** are diagonal: $\forall i \neq j$, $m_{ij} = 0$, $d_{ij} = 0$, and $a_{ij} = 0$.

If the center of mass of the stator lies on the rotor rotation axis and coincides with the center of mass of the balanced rotor, i.e., the condition is satisfied

$$x_D = y_D = z_D = 0, \quad (13)$$

and the inertia matrix **M** has a diagonal form:

$$\mathbf{M} = diag\{m, m, m, J_x, J_y, J_z, m_r, m_r\}, \quad (14)$$

where $m = m_s + m_r$ – the mass of the rotor-stator system; $J_x = J_{sx} + J_{rx}$, $J_x = J_{sy} + J_{ry}$, and $J_z = J_{sx} + J_{rx}$ – moments of inertia of the rotor-stator system with respect to coordinate axes.

If condition (13) is not satisfied, the matrix **M** contains off-diagonal elements: static mass moments with respect to coordinate axes m_{ij}, $i, j \leq 3$, $i \neq j$, and centrifugal moments of inertia m_{ij}, ($3 < i \leq 6$, $j \leq 6$, $i \neq j$).

The diagonal stiffness matrix **A** has the form:

$$\mathbf{A} = diag\{\sum_{i=1}^n c_{sx_i}, \sum_{i=1}^n c_{sy_i}, \sum_{i=1}^n c_{sz_i}, \\ \sum_{i=1}^m\left(c_{sz_i}y_i^2 + c_{sy_i}z_i^2\right), \sum_{i=1}^m\left(c_{sx_i}z_i^2 + c_{sz_i}x_i^2\right), \\ \sum_{i=1}^m\left(c_{sy_i}x_i^2 + c_{sx_i}y_i^2\right), \sum_{i=1}^m c_{rx_i}, \sum_{i=1}^m c_{rz_i}\}, \quad (15)$$

where $c_{sx_i}, c_{sy_i}, c_{sz_i}$ – the stiffness projections of n stator supports ($i = 1 \ldots n$); c_{rx_i}, c_{rz_i} – projections of stiffnesses of rotor supports ($i = 1, 2$).

Elements a_{ii} ($i \le 3$) are total stiffnesses of stator supports, a_{ii}; ($3 < i \le 6$) – torsional stiffnesses of stator supports; a_{ii} ($i > 6$) – total stiffnesses of rotor supports. For the diagonal form of the stiffness matrix, it is necessary that the off-diagonal elements are equal to zero: static stiffness moments relative to the coordinate planes of the system a_{ij} ($i, j \le 3$, $i \ne j$) and centrifugal stiffness moments relative to pairs of coordinate planes a_{ij} ($3 < i, j \le 6$, $i \ne j$).

In [24], it is substantiated that these conditions are satisfied if the stator support system's stiffness center coincides with the center of inertia and the main stiffness axes of the supports coincide with the rotor's main central axes of the inertia.

The diagonal inertia matrix **D** has the form:

$$\boldsymbol{D} = diag\left\{\sum_{i=1}^{n} h_{sx_i}, \sum_{i=1}^{n} h_{sy_i}, \sum_{i=1}^{n} h_{sz_i}, \sum_{i=1}^{m}\left(h_{sz_i}y_i^2 + h_{sy_i}z_i^2\right), \sum_{i=1}^{m}\left(h_{sx_i}z_i^2 + h_{sz_i}x_i^2\right), \sum_{i=1}^{m}\left(h_{sy_i}x_i^2 + h_{sx_i}y_i^2\right), \sum_{i=1}^{m} h_{rx_i}, \sum_{i=1}^{m} h_{rz_i}\right\},$$

where $h_{sx_i}, h_{sy_i}, h_{sz_i}$ – the projections of the viscous friction constant n of the stator supports ($i = 1 \ldots n$); h_{rx_i}, h_{rz_i} – the projections of the viscous friction constant of the rotor supports ($i = 1, 2$).

The elements d_{ii} – total damping coefficients of stator supports ($i \le 3$); d_{ii} – torsional damping coefficients of stator supports ($3 < i \le 6$); d_{ii} – total damping coefficients of rotor supports ($i > 6$).

For the diagonal form of the stiffness matrix, the off-diagonal elements must be equal to zero: static moments of viscous friction with respect to coordinate planes of the system d_{ij} ($i, j \le 3$, $i \ne j$) and centrifugal moments of viscous friction with respect to pairs of coordinate planes d_{ij} ($3 < i, j \le 6$, and $i \ne j$).

These conditions are satisfied if the principal axes of the stator support's viscous friction constants coincide with the stator's principal central axes of inertia [24].

The components and moments of the perturbing force of vector **Q** are equal to:

$$\begin{gathered} F_x = m_r\omega^2 e_U \sin\omega t; F_y = 0; \\ F_z = \boldsymbol{m_r\omega^2 e_U \cos\omega t}; \\ \boldsymbol{M_x = m_r\omega^2 e_U y_D \cos\omega t}; \\ \boldsymbol{M_y} = m_r\omega^2 e_U(z_D \sin\omega t - x_D \cos\omega t); \\ M_z = -m_r\omega^2 e_U y_D \sin\omega t, \end{gathered} \qquad (16)$$

where the forces F_x, F_y, and F_z – projections of the radial unbalanced force $F = m_r\omega^2 e_U$, caused by mechanical eccentricity; the moments M_x, M_y, and M_z – torques with respect to the coordinate axes, that arise in case of a mismatch of the rotor rotation axis with the stator central axis of inertia ($x_D \ne 0$, $z_D \ne 0$) and displacement of the rotor center of mass along the rotation axis ($y_D \ne 0$).

3.7 Mathematical model of motor vibrations with magnetic rotor eccentricity

Mixed magnetic eccentricity e_m is a combination of magnetic static and magnetic dynamic eccentricities. In general, it is not equal to the mass eccentricity e_U because it characterizes the deviation of the magnetic centers of the stator and rotor, which may not coincide with the geometric center of the stator and the rotor rotation axis, respectively.

Thus, static magnetic eccentricity e_{ms} creates a load on the rotor, which the resultant radial force can characterize F^s_{UMP}, which acts on the minimum air gap. The value of the static magnetic eccentricity is equal to the distance OD between the stator axis of inertia and the rotor axis of rotation in Fig. 1 is $e_{ms} = \sqrt{x_D^2 + z_D^2}$. The dynamic eccentricity e_{md} creates a force vector F^d_{UMP}, which acts on the rotor and rotates at the rotor speed.

Since UMP does not depend on the parameters included in the model (12), the influence of UMP can be accounted for by the additional radial nonlinear force F_{UMP} and its moments in (12). Under the assumption of constant angular speed $\omega = \text{const}$), the theoretical expressions proposed in [4, 11] can be applied can be applied to estimate the UMP force (Fig. 4).

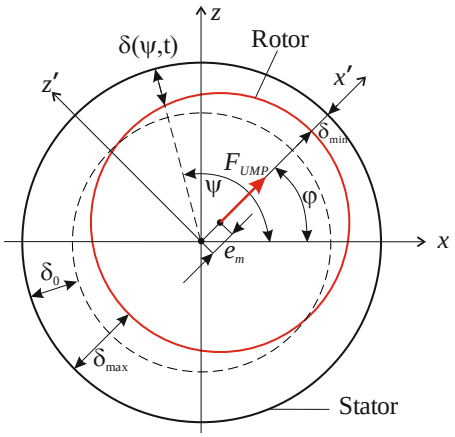

Figure 4 – Diagram of the magnetic eccentricity of the rotor

The value of the air gap of the eccentric rotor for an arbitrary eccentricity at any time is approximated:

$$\delta(\psi, t) \approx \delta_0 - e_m(t)\cos[\psi - \varphi(t)], \qquad (17)$$

where δ_0 – the average value of air gap at rotor centering; ψ – the stator position angle; $e_m(t)$ – the value of magnetic eccentricity at time t; $\varphi(t)$ is the position angle of eccentricity (rotation of the rotor center) at time t.

At static eccentricity e_{ms}, the air gap at an arbitrary point on the inner surface of the stator is defined as

$$\delta(\psi) \approx \delta_0 - e_{ms}\cos(\psi - \varphi), \qquad (18)$$

where φ – the position angle of static eccentricity.

At dynamic eccentricity e_{md}, the eccentricity position angle is a function of time $\varphi(t) = \varphi_0 + \omega t$, therefore

$$\delta(\psi, t) \approx \delta_0 - e_{md}\cos(\psi - \varphi_0 - \omega t), \qquad (19)$$

where φ_0 – the initial position angle of the dynamic eccentricity; ω – the angular speed of rotor rotation.

UMP is highly nonlinear. Nonlinear methods of UMP calculation use the energy method or integration of the Maxwell stress tensor in the air gap between the stator and rotor [10]. The expression for the unbalanced magnetic pull on the rotor surface is defined as

$$\begin{gathered} F_{UMPx} = f_1 \cos\varphi + f_2 \cos(2\omega_e t - \varphi) + \\ + f_3 \cos(2\omega_e t - 3\varphi), p = 1, \\ f_1 \cos\varphi + f_3 \cos(2\omega_e t - 3\varphi) + \\ + f_4 \cos(2\omega_e t - 5\varphi), p = 2, \\ f_1 \cos\varphi + f_4 \cos(2\omega_e t - 5\varphi), p = 3, \\ f_1 \cos\varphi, p \geq 4; \\ F_{UMPz} = f_1 \sin\varphi + f_2 \sin(2\omega_e t - \varphi) + \\ + f_3 \sin(2\omega_e t - 3\varphi), p = 1, \\ f_1 \sin\varphi + f_3 \sin(2\omega_e t - 3\varphi) + \\ + f_4 \sin(2\omega_e t - 5\varphi), p = 2, \\ f_1 \sin\varphi + f_4 \sin(2\omega_e t - 5\varphi), p = 3, \\ f_1 \sin\varphi, p \geq 4, \end{gathered} \tag{20}$$

where F_{UMPx} and F_{UMPz} – projections of the magnetic pull force on the x and z axes, respectively; ω_e – the angular frequency of the stator winding power supply source; p is the number of pole pairs of stator windings; f_1, f_2, f_3, f_4 – the amplitudes of the components of the UMP:

$$\begin{gathered} f_1 = 0.25Rl\pi\mu_0^{-1}F_j^2(2\Lambda_0\Lambda_1 + \Lambda_1\Lambda_2 + \Lambda_2\Lambda_3); \\ f_2 = 0.25Rl\pi\mu_0^{-1}F_j^2\left(\Lambda_0\Lambda_1 + \frac{1}{2}\Lambda_1\Lambda_2 + \frac{1}{2}\Lambda_2\Lambda_3\right); \\ f_3 = 0.25Rl\pi\mu_0^{-1}F_j^2\left(\Lambda_0\Lambda_3 + \frac{1}{2}\Lambda_1\Lambda_2\right); \Lambda_2\Lambda_3, \\ f_4 = 0.125Rl\pi\mu_0^{-1}F_j^2, \end{gathered} \tag{21}$$

where R – the rotor radius; l – the rotor length; F_j – the amplitude of the fundamental wave of magnetomotive force (MMF) of rotor excitation; μ_0 – the air permeance; Λ_i – the Fourier coefficients in the expression of the magnetic permeability of the air gap:

$$\Lambda_i = \begin{cases} \frac{\mu_0}{\delta_0}\frac{1}{\sqrt{1-\varepsilon^2}}, i = 0; \\ \frac{2\mu_0}{\delta_0}\frac{1}{\sqrt{1-\varepsilon^2}}\left(\frac{1}{1+\sqrt{1-\varepsilon^2}}\right)^i, i > 0, \end{cases} \tag{22}$$

where $\varepsilon = e_m / \delta_0$ – relative eccentricity.

The angular speed of rotation of the rotor, considering the slip s of the IM, is related to the angular speed of rotation of the magnetic field ω_m and the angular frequency of the electric current supplying the winding ω_e as follows:

$$\omega = (1-s)\omega_m = (1-s)\frac{\omega_e}{p}. \tag{23}$$

The resultant magnetic tension force F_{UMP} is defined as a vector sum of forces $\bar{F}_{UMP} = \bar{F}^s_{UMP} + \bar{F}^d_{UMP}$. To consider the rotor's mechanical and magnetic eccentricity, the vector of magnetic force factors $\mathbf{Q}_{UMP}$ should also be added to the vector $\mathbf{Q}$ of the system (12).

Thus, equation (12) takes the following form:

$$\mathbf{M}\ddot{\mathbf{q}} + (\mathbf{G}+\mathbf{D})\dot{\mathbf{q}} + \mathbf{A}\mathbf{q} = \mathbf{Q} + \mathbf{Q}_{UMP}, \tag{24}$$

where $\mathbf{Q}_{UMP} = [F_{UMPx}, 0, F_{UMPz}, M_{UMPx}, M_{UMPy}, M_{UMPx}, M_{UMPz}, F_{UMPx}, F_{UMPz}]^T$.

Denoting the magnetic center of the rotor as $D^m(x_D, y_D^m, z_D)$, the moments of the unbalanced tension force can be determined analogously (Fig. 5):

$$\begin{gathered} M_{UMPx} = F_{UMPz} y_D^m; \\ M_{UMPy} = F_{UMPx} z_D - F_{UMPz} x_D; \\ M_{UMPz} = -F_{UMPx} y_D^m, \end{gathered} \tag{25}$$

where y_D^m – the axial displacement of the rotor magnetic center is generally not equal to the axial displacement of the rotor mass center y_D.

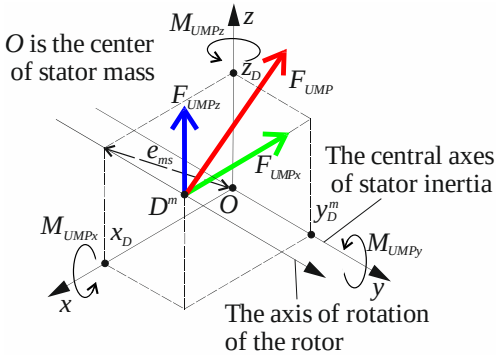

Figure 5 – Diagram of the UMP force and its moments

4 Results

4.1 Refinement of elastic-inertia and damping parameters of the model

An 11 kW IM with a squirrel cage rotor with an allowable vibration displacement level of 70 μm was selected for modeling. The motor is used in metalworking and woodworking machines, as well as in fans, pumps, and other industrial systems. The main characteristics of the IM are given in Table 1.

The accuracy and reliability of modeling significantly depend on the way of installation of the IM and the accuracy of values of elastic-inertial and damping characteristics of the system, so let us consider in detail the process of their selection.

The IM under consideration is fixed to the foundation by means of "feet". The stator supports are bolted connections between the stator feet and the foundation. The diameter of the bolts is 10 mm. The international standards ISO 10816 and IEC 60034-14 regulate the stiffness of IM foundations: foundations must be designed so that their critical frequency lies above the IM operating frequency and 2 times the supply frequency for 2nd-pole IMs. The stiffness of such foundations should be greater than $1 \cdot 10^9$ N/m. In practice, achieving these values with steel foundations is often impossible. The actual stiffness of this type of IM foundation is much lower at 10^8 N/m. This stiffness value can be assumed to be the vertical stiffness of the support c_{sz}. The stiffness of supports in the horizontal plane is determined by the stiffness of bolted connections and was calculated according to the methodology described in [25]. The elastic characteristics of bolted connections were considered linear. The calculated values of stator support stiffnesses c_{sx}, c_{sy} are given in Table 1.

Table 1 – Parameters of the three-phase induction motor

Notation	Description	Value
Motor data		
n	Rated speed, rpm	3000
s	Rated slip	0.033
R	Radius of the rotor, mm	63.5
l	Length of the rotor, mm	130
m_r	Mass of the rotor, kg	14.22
m_s	Mass of the stator, kg	57.78
δ_0	Mean air-gap length, mm	0.45
μ_0	Air permeance, N/m	$4\pi \cdot 10^{-7}$
F_j	Fundamental MMF amplitude of the rotor excitation current, A	945
p	Number of pole pairs	1
c_{rx}, c_{rz}	Stiffness of bearing housing and end shield, N/m	$5.52 \cdot 10^7$
e	Permissible eccentricity (μm)	20
y_1, y_2	Coordinates y of rotor bearing connection points (mm)	(–65, 65)
Foundation data		
c_{sz}	Vertical stiffness of the foundation at each motor support (N/m)	$2.5 \cdot 10^7$
c_{sx}, c_{sy}	Horizontal stiffness of the foundation at each motor support (N/m)	$2 \cdot 10^8$
$tg(\delta_s)$	Mechanical loss factor of the foundation	0.08
x_i	Coordinates of stator support connection points, mm (i = 1, 2, …, 4)	(–108, 108, 108, –108)
y_i		(–89, –89, 89, 89)
z_i		(–132, –132, –132, –132)

The rotor supports are 6208 ZZ-C3 rolling ball bearings seated in cast iron bearing shields. Assuming that the cast iron bearing shields are non-deformable, the stiffness of the rotor supports is entirely determined by the radial stiffness of the bearings. In general, the radial stiffness of the bearings is nonlinear, as it depends on the bearing load and its radial clearance. The radial stiffness of the bearing can be calculated using the methodology described in [26]:

$$c_r = 8.41 \cdot 10^6 \cdot \sqrt[3]{DQz^2 \cos^5 \alpha}, \qquad (26)$$

where z – the number of rolling elements; D – the diameter of the ball, m; Q – the equivalent dynamic radial load, N; α – the contact angle, rad.

In the ideal case, when there is no mass unbalance, the radial load is determined only by the weight of the rotor, and the bearing stiffness calculated by formula (26) is $4.93 \cdot 10^7$ N/m.

In case of imbalance, the dynamic load will increase, and the bearing stiffness will increase. Let's the rotor be pre-balanced, and the vibration amplitude does not exceed 70 μm (under the recommendations of the international standard ISO 20816-1:2016 "Mechanical vibration. Measurement and evaluation of machine vibration. Part 1: General guidelines").

In this case, the mechanical unbalance of the rotor is 0.28 g·mm, which corresponds to the eccentricity e_U = 20 μm. At rotation of the rotor with operating speed ω = 314 rad/s due to the mass eccentricity, there is an additional radial unbalanced force with an amplitude of $F = m_2 e_U \omega^2$ = 28 (N). Thus, the equivalent dynamic radial load on the bearing without considering axial load and the rotor gravity force is equal to Q = 97.6 N, and the bearing stiffness increases by 12 %: $c_r = 5.52 \cdot 10^7$ N/m.

The model (24) analysis shows that the pliability of the considered bearings in the frequency range from 0 to 1000 rad/s does not affect the appearance of dangerous resonances in the system. The change of bearing stiffness at load change, according to (26), does not significantly influence the frequency response of the IM. The stiffness of the stator supports determines the motor case's 1st critical speed.

The damping coefficients h_{rx_i}, h_{rz_i} $(i = 1, 2)$ of the bearing housing (rotor supports) can be calculated as $2.5 \cdot 10^{-5} c_r$ [27]. The damping coefficients of the stator supports were determined according to the method described in [17]. The damping coefficients $h_{sx_i}, h_{sy_i}, h_{sz_i}$ $(i = 1, 2, 3, 4)$ of the supports can be calculated by the mechanical loss factor $tg(\delta_s)$:

$$h_s = \frac{c_s \, tg(\delta_s)}{\omega}. \qquad (27)$$

The simulation was carried out using the MATLAB Simulink. The Runge-Kutta approach is applied to solve the system of differential equations (24). The block diagram of the calculation algorithm is presented in Fig. 6.

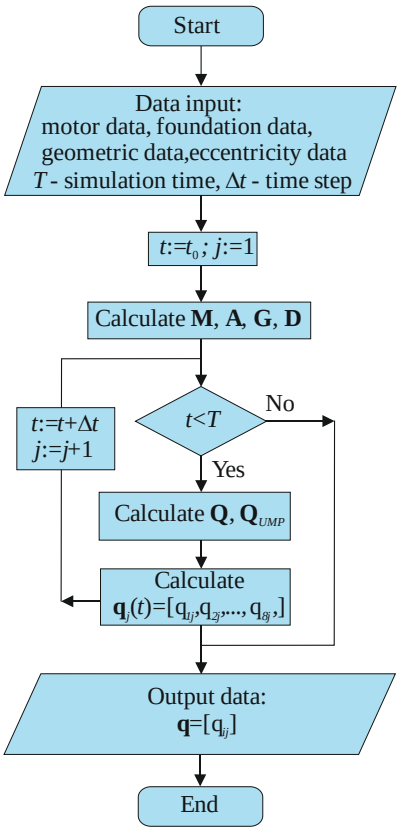

Figure 6 – Block diagram of the calculation process

4.2 Analysis of critical frequencies

Consider the transverse vibrations of the IM, whose rotor is characterized by mass eccentricity. The value of the critical frequencies of the IM is influenced by the pliability of the stator supports. In general, the stator has 6 critical frequencies. In particular, transverse vibrations of the stator are characterized by critical frequencies f_{csx} = 117.6 Hz, f_{csz} = 183.2 Hz, and axial – f_{csy} = 99.9 Hz. Critical frequencies of the rotor are equal to f_{crx} = 132.9 Hz, f_{crz} = 184.1 Hz.

The design of this IM is such that the static and centrifugal stiffness and viscous friction moments are not zero because the coordinate planes about which they are defined are not the symmetry planes of the stator support system. The stiffness matrix **A** and the damping matrix **D** are non-diagonal. Fig. 7 demonstrates the dependence of the amplitude of transverse horizontal vibrations on the frequency at different values of the rotor height above the connection points of the coordinate supports z = {0, 30, 60, 100, 132} mm.

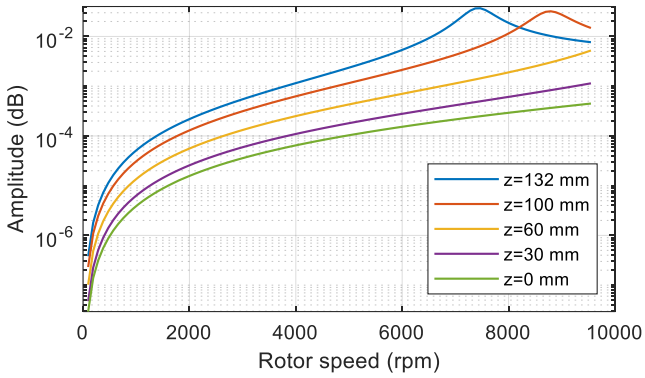

Figure 7 – Frequency response of stator vibration amplitude

The results show that to reduce the IM's vibration activity, the best design solution would be to position the stator supports in the *xOy* plane.

Another solution is to add additional supports symmetrically to the existing ones with respect to the rotor axis, placing them in the horizontal plane at a distance z = 132 mm from the rotor axis.

Fig. 8 shows the comparative dependences of horizontal transverse vibrations of the rotor at different types of eccentricity: mass eccentricity e_U = 20 μm; static magnetic eccentricity e_{ms} = 4.5 μm (ε = 0.01); the angle φ = 0; dynamic magnetic eccentricity e_{ms} = 4.5 μm (ε = 0.01).

Fig. 8 shows that the IM has two critical velocities. The first is caused by static magnetic eccentricity and the second is caused by mass eccentricity. Static magnetic eccentricity leads to the appearance of another critical velocity on the frequency response, the value of which is approximately 2 times smaller. Thus, even an IM with a perfectly balanced rotor with zero mass unbalance due to its eccentric position in the stator bore always has a critical frequency caused by static magnetic eccentricity. Since the F_{UMP} force varies with twice the frequency compared to the current frequency ω_e (at p = 1), this frequency is about 2 times the rotor speed. The UMP spectrum contains zero frequency and $2\omega_e$ frequency components.

When the rotational speed is reached $0.5(1-s)\omega_{cr_U}$, an unbalanced magnetic force acts on the rotor with frequency ω_{cr_U}. This gives the IM another critical speed ω_{cr_m}, which for an arbitrary number of pole pairs p is defined as follows:

$$\omega_{cr_m} = \frac{(1-s)}{2p}\omega_{cr_U}. \qquad (28)$$

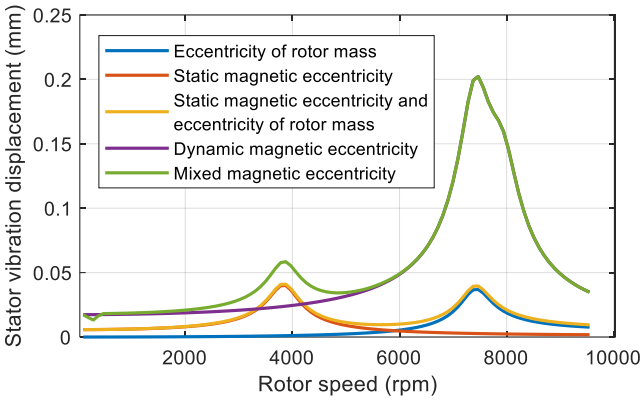

Figure 8 – Comparative dependences of horizontal stator vibrations at different types of rotor eccentricity

5 Discussion

The danger of static magnetic eccentricity is that even if the critical frequencies lie above the motor operating frequencies, UMP can lead to the appearance of resonance in the operating frequency zone. The results obtained agree with those obtained by other authors [28–31].

In known models, the mass eccentricity e_U is only considered when calculating the unbalanced radial force $F = m_r\omega^2 e_U$. The results show that due to the mismatch between the axis of rotation and the central axis of inertia of the stator, taking into account in the model the change of the motor moments of inertia by the values of moments of inertia $J_x = m_r(y_D^2 + z_D^2)$, $J_y = m_r(z_D^2 + x_D^2)$, and $J_z = m_r(x_D^2 + y_D^2)$ increase the accuracy of modeling. Particularly, at an axial displacement of the magnetic center relative to the central axis of symmetry of the stator by 10 mm, the moments of inertia of the motor relative to the x and z axes increase by 0.2 %. Although the effect seems negligible, the model also accounts for the effect of torques that create additional critical velocities for rotational motion. Knowledge of the natural frequency spectrum of the motor system seems to be very important.

Attention should also be paid to the additional increase in static magnetic eccentricity due to the increase in bearing clearance caused by dynamic loading. In the known models in publications [3, 15–17, 28, 29], the magnitude of magnetic eccentricity is analyzed without considering the change in bearing radial clearance. The radial clearance in the bearing is made up of elastic deformations and the nameplate clearance.

At low bearing loads, elastic deformations are insignificant and are neglected, assuming that the radial clearance corresponds to the nameplate value. Under the influence of magnetic attraction, the radial clearance of the bearing and the clearances between the outer surface of the bearing ring and the inner surface of the shield, as well as between the shield and the bed in the place of shield seating, are selected. When a load is applied to the bearing, it elastically deforms, increasing the internal clearance. The relationship between the radial load and the deformation clearance of a ball bearing is determined by the relationship established based on the Hertz theory [30]:

$$\Delta = 1.285 \cdot 10^{-3} \cdot \sqrt[3]{\frac{Q^2}{Di^2 z^2 \cos^5 \alpha}}, \qquad (29)$$

where i – the number of bearing rows.

For the example under consideration, at the operating frequency with permissible eccentricity, the radial displacement of the inner and outer ring of the bearing is Δ = 5.75 μm. At the maximum value of the radial force at the critical frequency, the radial displacement will be Δ = 13.4 μm. Consequently, adding up with the initial static magnetic eccentricity, the resulting value of magnetic eccentricity will increase. For the IM we have considered, this increase in magnetic eccentricity is 3% of the air gap with an accepted allowable relative eccentricity of 10 %. Thus, the error in determining the allowable eccentricity can reach 30 %.

However, some authors, for example, in [29], draw attention to the problem of determining the actual static eccentricity during the system assembly. We believe that the eccentricity value should be determined in dynamics, considering the actual deformation clearance of the bearings. The solution to this problem can become the basis for future research.

The analysis of dependence (25) has shown that the increase of F_{UMP} at resonance leads to the increase of rotor bearing stiffness up to $8.57 \cdot 10^7$ N/m and, accordingly, to the decrease of stator vibrations, but this effect is insignificant (2–3 %).

The known models [1-10, 28] do not consider the influence of such parameters: the axial displacement of the center of inertia y_D and the magnetic center of the rotor y_D^m. Usually, the authors explain it by saying that their influence is insignificant. Our simulation results show that considering these coordinates is necessary for more accurate vibration results. In real IMs, both the unbalanced force F and the magnetic pull force F_{UMP} do not lie in the OXZ plane passing through the stator center of inertia.

The developed model allowed for investigating the influence of the longitudinal displacement y_D of the rotor center of mass and the axial displacement of the rotor magnetic center. Fig. 9 shows the frequency dependencies of the axial vibration magnitude obtained at different values of the coordinate y_D^m.

This is explained by an increase in the moment of action of the UMP, which leads to an increase in angular oscillations relative to the x and z axes due to the action of torques M_{UMPx} and M_{UMPz} along the coordinates α and γ.

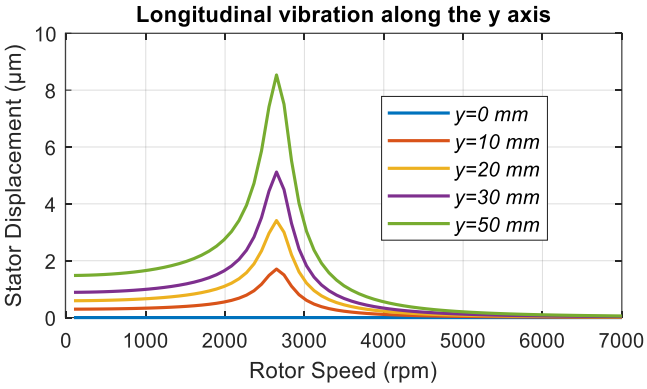

Figure 9 – Frequency response at variable displacement y_D^m (axial vibrations)

An increase in angular vibrations causes an increase in the displacement of the stator due to the translational and rotational movement. These vibrations can negatively affect the performance of the bearing node and reduce its service life.

In [10, 29], attention was paid to the dependence of the magnitude of magnetic tension on the position of the minimum air gap. Our simulation results also showed a significant influence of the direction of the smallest air gap on the magnitude of vibrations. Fig. 10 shows the distribution of the amplitude of transverse horizontal vibrations from frequency when the angle φ of static eccentricity is changed.

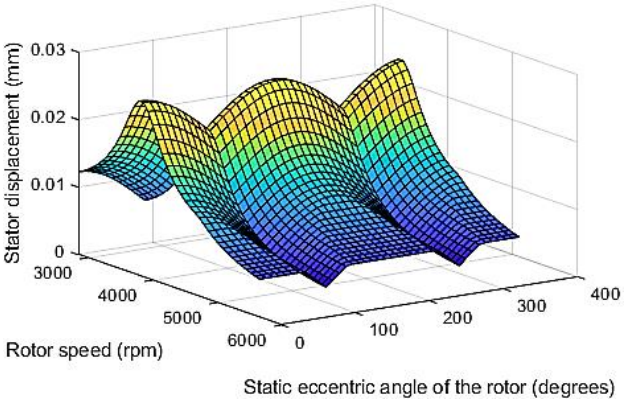

a

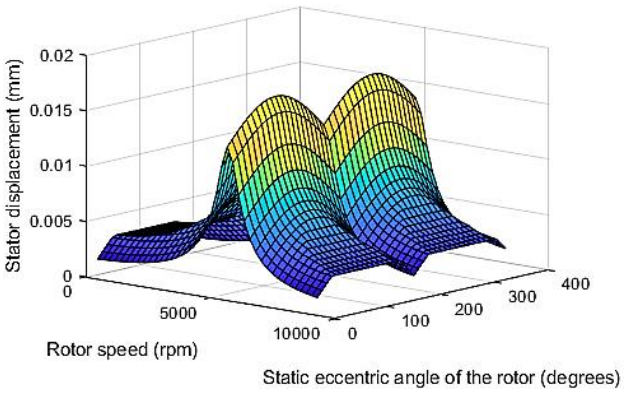

b

Figure 10 – Dependence of stator vibrations on the eccentricity angle at static magnetic eccentricity: a – horizontal vibrations; b – vertical vibrations

The horizontal vibrations along the *x*-axis are maximum at $\varphi = 0°$ and $\varphi = 180°$, when $F_{UMPx} \to \max$, $F_{UMPz} \to 0$. The vibrations along the *x*-axis are minimum at $\varphi = 90°$ and $\varphi = 270°$, when $F_{UMPx} \to 0$, $F_{UMPz} \to \max$.

Vertical vibrations along the *z*-axis are maximum at $\varphi = 90°$ and $\varphi = 270°$, when $F_{UMPz} \to \max$, $F_{UMPx} \to 0$. Vibrations along the *z*-axis are minimum at $\varphi = 0°$ and $\varphi = 180°$, when $F_{UMPx} \to \max$, $F_{UMPz} \to 0$.

Static balancing of a rigid rotor in two correction planes will not reduce the unbalance due to magnetic eccentricity. The angle of magnetic eccentricity should always be considered to improve balancing efficiency.

6 Conclusions

A mathematical model of the dynamics of an induction motor with 8 degrees of freedom has been created. The model allows for eccentricity of the rotor mass, the static and dynamic magnetic eccentricity of the rotor, the influence of the gyroscopic moment of the rotor, and unequal stiffness of the stator and rotor supports and their number and places of connection.

The model differs in considering the influence of the rotor's eccentric position in the stator bore, axial deviation of mass, and magnetic unbalance from the stator center of mass. For this purpose, degrees of freedom for the rotational motion of the stator and longitudinal translational motion of the stator are introduced into the model. The main results of this study can be summarized as follows.

First, consideration of the moments of mass and electromagnetic unbalanced forces and additional degrees of freedom allows for modeling the rotor and stator axial vibrations. The magnitude of axial vibrations increases with increasing distance between the center of inertia of the stator, the center of inertia of the rotor, and the magnetic center of the rotor.

Also, static magnetic eccentricity causes an additional critical motor speed, which decreases in proportion to the increase in the number of pole pairs. The danger of static magnetic eccentricity is that even if the critical frequencies lie above the operating frequencies of the motor, the unbalanced magnetic pull can lead to resonance in the operating frequency zone.

Moreover, the static magnetic eccentricity can increase further at IM operating frequencies due to the increase in bearing clearance caused by dynamic unbalanced loading. The possible error in determining the permissible eccentricity without considering the change in bearing radial clearance can reach 30 %.

Finally, the angle of static magnetic eccentricity significantly affects the magnitude of transverse vibrations. This feature should be considered when balancing rotors when selecting the locations of balancing weights.

References

1. Popa, L. M., Jensen, B. B., Ritchie, E., Boldea, I. (2003). Condition Monitoring of Wind Generators. *In: 38th IAS Annual Meeting on Conference Record of the Industry Applications Conference*. Salt Lake City, UT, USA, Vol. 3, pp. 1839–1846. https://doi.org/10.1109/IAS.2003.1257819
2. Thomson, W. (2020). Vibration Monitoring of Induction Motors and Case Histories on Shaft Misalignment and Soft Foot. *In Vibration Monitoring of Induction Motors: Practical Diagnosis of Faults via Industrial Case Studies*. Cambridge University Press, Cambridge, UK. https://doi.org/10.1017/9781108784887.002
3. Liu, Y., Chen, Z., Hua, X., Zhai, W. (2022) Effect of rotor eccentricity on the dynamic performance of a traction motor and its support bearings in a locomotive. *Proceedings of the Institution of Mechanical Engineers, Part F: Journal of Rail and Rapid Transit*, Vol. 236(9), pp. 1080–1090. https://doi.org/10.1177/09544097211072335
4. Michon, M., Holehouse, R. C., Atallah, K., Johnstone, G. (2014). Effect of rotor eccentricity in large synchronous machines. *IEEE Transactions on Magnetics*, Vol. 50(11), 8700404. https://doi.org/10.1109/TMAG.2014.2330452
5. Richard N. Bell et al. (1985) Report of large motor reliability survey of industrial and commercial installations, Part II. *IEEE Transactions on Industry Applications*, Vol. 21(4), pp. 865–872. https://doi.org/10.1109/TIA.1985.349533
6. Cornell, E. P., Owen, E. L., Appiarius, J. C., McCoy, R. M., Albrecht, P. F., and Houghtaling, D. W. (1982). *Improved Motors for Utility Applications. Final Report.* U.S. Department of Energy, Office of Scientific and Technical Information United States, Oak Ridge, TN, USA. https://doi.org/10.2172/6759687
7. Bellini, A., Immovilli, F., Rubini, R., Tassoni, C. (2008). Diagnosis of bearing faults of induction machines by vibration or current signals: A critical comparison. *In: 2008 IEEE Industry Applications Society Annual Meeting*. Edmonton, AB, Canada, 2008, pp. 1–8. https://doi.org/10.1109/08IAS.2008.26
8. Chuan, H., Shek, J. K. (2018). Calculation of unbalanced magnetic pull in induction machines through empirical method. *IET Electric Power Applications*, Vol. 12(9), pp. 1233–1239. https://doi.org/10.1049/iet-epa.2018.0085
9. Salah, A. A., Dorrell, D. G., Guo, Y. (2019). A Review of the monitoring and damping unbalanced magnetic pull in induction machines due to rotor eccentricity. *IEEE Transactions on Industry Applications*, Vol. 55(3), pp. 2569–2580. https://doi.org/10.1109/TIA.2019.2892359
10. Dorrell, D. G., Hsieh, M., Guo, Y. (2009). Unbalanced magnet pull in large brushless rare-earth permanent magnet motors with rotor eccentricity. *IEEE Transactions on Magnetics*, Vol. 45, pp. 4586–4589. https://doi.org/10.1109/TMAG.2009.2022338

11. Burakov, A., Arkkio, A. (2007). Comparison of the unbalanced magnetic pull mitigation by the parallel paths in the stator and rotor windings. *IEEE Transactions on Magnetics*, Vol. 43(12). pp. 4083–4088. https://doi.org/10.1109/TMAG.2007.906885
12. Zhu, Z. Q., Ishak, D., Howe, D., Chen, J. (2007). Unbalanced magnetic forces in permanent-magnet brushless machines with diametrically asymmetric phase windings. *IEEE Transactions on Industry Applications*, Vol. 43(6). pp. 1544–1553. https://doi.org/10.1109/TIA.2007.908158
13. Dorrell, D. G., Hsieh, M. F. (2010). Calculation of radial forces in cage induction motors at start – The effect of rotor differential. *IEEE Transactions on Magnetics*, Vol. 46(8), pp. 3029–3032. https://doi.org/10.1109/TMAG.2010.2044389
14. Liu, F., Xiang, C., Liu, H., Chen, X., Feng, F., Cong, H., Kuilong, Yu. (2022). Model and experimental verification of a four degrees-of-freedom rotor considering combined eccentricity and electromagnetic effects. *Mechanical Systems and Signal Processing*, Vol. 169, 108740. https://doi.org/10.1016/j.ymssp.2021.108740
15. Werner, U. (2017) Influence of the foundation on the threshold of stability for rotating machines with roller bearings – A theoretical analysis. *Journal of Applied Mathematics and Physics*, Vol. 5, pp. 1380–1397. https://doi.org/10.4236/jamp.2017.56114
16. Werner, U. (2017). Mathematical multibody model of a soft mounted induction motor regarding forced vibrations due to dynamic rotor eccentricities considering electromagnetic field damping. *Journal of Applied Mathematics and Physics*, Vol. 5(2), pp. 346–364. https://doi.org/10.4236/jamp.2017.52032
17. Werner, U. (2017). Influence of electromagnetic field damping on forced vibrations of induction rotors caused by dynamic rotor eccentricity. *ZAMM-Journal of Applied Mathematics and Mechanics*, Vol. 97(1), pp. 38–59. https://doi.org/10.1002/zamm.201500285
18. Jiang, J. W., Bilgin, B., Sathyan, A., Dadkhah, H., Emadi, A. (2016). Analysis of unbalanced magnetic pull in eccentric interior permanent magnet machines with series and parallel windings. *IET Electric Power Applications*, Vol. 10(6), pp. 526–538. https://doi.org/10.1049/iet-epa.2015.0186
19. Calleecharan, Y., Jauregui, R., Aidanpää, J.-O. (2013). Towards a general method for estimating the unbalanced magnetic pull in mixed eccentricities motion including sufficiently large eccentricities in a hydropower generator and their validation against EM simulations. *The European Physical Journal Applied Physics*, Vol. 63(2), 20901. https://doi.org/10.1051/epjap/2013130092
20. Wu, B., Sun, W., Li, Z., Li, Z. (2011). Circular whirling and stability due to unbalanced magnetic pull and eccentric force. *Journal of Sound and Vibration*, Vol. 330(21), pp. 4949–4954. https://doi.org/10.1016/j.jsv.2011.05.028
21. Du, J., Li, Y. (2023). Analysis on the Variation laws of electromagnetic force wave and vibration response of squirrel-cage induction motor under rotor eccentricity. *Electronics*, Vol. 12(6), 1295. https://doi.org/10.3390/electronics12061295
22. Lei, A., Song, C.-X., Lei, Y.-L., Fu, Y. (2021). Design optimization of vehicle asynchronous motors based on fractional harmonic response analysis. *Mechanical Sciences*, Vol. 12, pp. 689–700. https://doi.org/10.5194/ms-12-689-2021
23. Essen, H. (1993). Average angular velocity. *European Journal of Physics*, Vol. 14(5), 201. https://doi.org/10.1088/0143-0807/14/5/002
24. Drach, I., Goroshko, A., Dwornicka, R. (2021). Design principles of horizontal drum machines with low vibration. *Advances in Science and Technology Research Journal*, Vol. 15(2), pp. 258–268. https://doi.org/10.12913/22998624/136441
25. Brown, K. H., Morrow, C. W., Durbin, S. G. (2008). *Guideline for Bolted Joint Design and Analysis: Version 1.0*. Sandia Report SAND2008-0371. Sandia National Laboratories, Albuquerque, NM, USA. https://doi.org/10.2172/929124
26. Gargiulo, E. P. (1980). A simple way to estimate bearing stiffness. *Machine Design*, Vol. 52(17). pp. 107–110.
27. Krämer, E. (1993). *Dynamics of Rotors and Foundations*. Springer-Verlag Berlin Heidelberg GmbH, Berlin, Germany.
28. Kim, H., Sikanen, E., Nerg, J., Sillanpää, T., Sopanen, J. T. (2020). Unbalanced magnetic pull effects on rotordynamics of a high-speed induction generator supported by active magnetic bearings – Analysis and experimental verification. *IEEE Access*, Vol. 8, pp. 212361–212370. https://doi.org/10.1109/ACCESS.2020.3039629
29. Kim, H., Nerg, J., Choudhury, T., Sopanen, J. T. (2020). Rotordynamic simulation method of induction motors including the effects of unbalanced magnetic pull. *IEEE Access*, Vol. 8, pp. 21631–21643. https://doi.org/10.1109/ACCESS.2020.2968915
30. Han, Y., Yang, L., Xu, T. (2021). Analysis of static stiffness fluctuation in radially loaded ball and roller bearings. *Archive of Applied Mechanics*, Vol. 91, pp. 1757–1772. https://doi.org/10.1007/s00419-020-01853-6
31. He, Y. L., Dai, D.-R., Xu, M.-X., Zhang, W., Tang, G.-J., Wan, S.-T., Sheng, X.-L. (2022). Effect of static/dynamic air gap eccentricity on stator and rotor vibration characteristics in doubly fed induction generator. *IET Electric Power Applications*, Vol. 16(11), pp. 1378–1394. https://doi.org/10.1049/elp2.12234